Available online at www.sciencedirect.com

ScienceDirect

Procedia Structural Integrity 2 (2016) 1229–1236

Structural Integrity Procedia

www.elsevier.com/locate/procedia

21st European Conference on Fracture, ECF21, 20-24 June 2016, Catania, Italy

Crack Propagation in Additive Manufactured Materials and Structures

Andre Riemer[a,b,*], Hans Albert Richard[a,b]

[a]Institute of Applied Mechanics, University of Paderborn, Pohlweg 47-49, 33098 Paderborn, Germany
[b]Direct Manufacturing Research Center DMRC, University of Paderborn, Mersinweg 3, 33100 Paderborn, Germany

Abstract

Additive manufacturing processes gain more and more interest, among others, due to the feasibility for production of lightweight metallic components directly from design data. Selective laser melting (SLM) is a very promising direct manufacturing (DM) technique for fabrication of near net shape components. The reasons for this are the relative high surface quality and bulk density of SLM processed parts. Still, process induced imperfections, i.e. residual stresses upon processing, need to be considered for future applications, in particular in the aerospace and biomedical sectors. Moreover, fatigue loading is a critical scenario for such components and needs to be investigated thoroughly.
In this paper, results from fatigue crack propagation tests on biocompatible SLM-materials (titanium alloy Ti-6-4 and stainless steel AISI 316L) will be presented. For that purpose, fracture mechanical analyses were carried out on these materials. For Ti-6-4 various treatments were taken into account. It could be shown, which optimization steps are required in order to achieve fracture mechanical properties that are comparable to the reference material. In case of 316L, crack growth data for different process parameter sets (different build-up rates) were examined and compared to make conclusions about the influence of increased build-up rate on resultant crack growth behavior. Finally, based on the insights deduced from foregoing tests on Ti-6-4 crack growth propagation and the lifetime were simulated numerically by the use of the software ADAPCRACK3D.

Keywords: Selective Laser Melting; titanium alloy Ti-6-4; stainless steel AISI 316L; threshold values of fatigue crack growth; *da/dN*-Δ*K*-curves; crack simulation in a hip joint implant

* Corresponding author. Tel.: +49 5254 6498453
E-mail address: andre.riemer@gmx.de

Copyright © 2016 The Authors. Published by Elsevier B.V. This is an open access article under the CC BY-NC-ND license (http://creativecommons.org/licenses/by-nc-nd/4.0/).
Peer review under responsibility of the Scientific Committee of ECF21.
10.1016/j.prostr.2016.06.157

1. Additive Manufacturing – innovative production technique with huge potential

The first efforts to develop Additive Manufacturing (AM) machines have been made in the 80s. These machines were characterized by low build-up rates and marginal process stability as well as inadequate surface quality and material properties, Levy et al. (2003). Since then, the development of these machines has been pushed continuously, Levy et al. (2003) and Kruth et al. (1998). For a long time this process has been mainly used for manufacturing of prototypes. The ongoing improvement and the promising outlook for the future, Gausemeier et al. (2011), as well as the unique capabilities of AM technique make them attractive for the aircraft and biomedical applications.

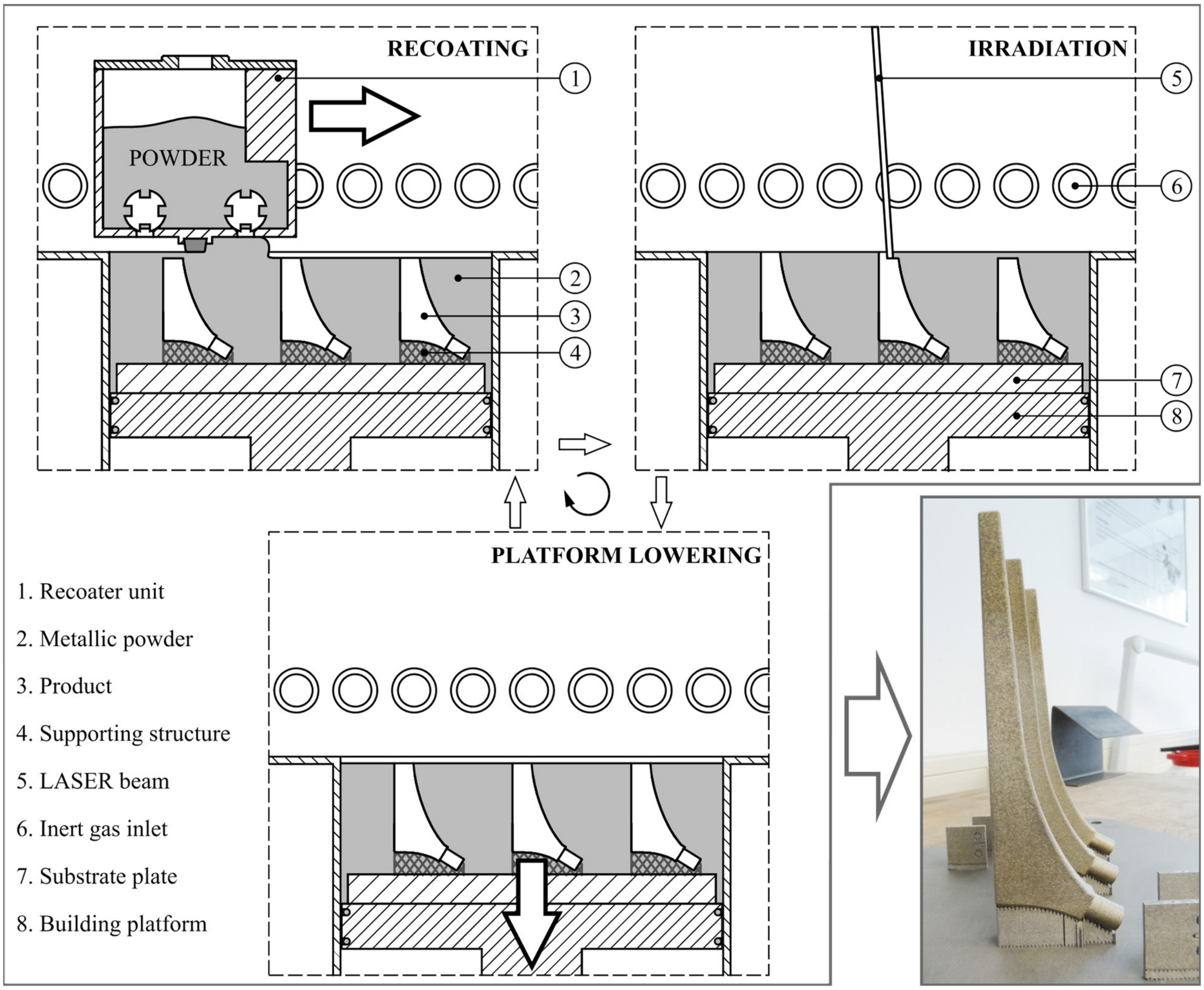

Fig. 1. Schematic of the SLM-process and 3 basic steps recoating, irradiation and platform lowering needed to produce a hip joint implant.

For all AM-processes is common that part production is based on the CAD model which has to be designed or obtained using 3D-scans in the step before manufacturing. The additive manufacturing process Selective Laser Melting (SLM) is characterized by transition of powdered material into solid part following being irradiated by the laser source, c.f. Fig. 1. The melt pool within this process is extended only in a small local area. Hence, layer-by-layer manufacturing of complex and delicate components becomes possible. The fabrication of parts by SLM is an iterative process that is divided in three consecutive steps, Fig. 1, as follows:

- RECOATING: This step involves the deposition of powder; either directly on the substrate plate within the first recoating step or on the previously deposited and irradiated powdered material in each subsequent step.
- IRRADIATION: Here, the powdered material becomes locally melted by the laser energy and bonded with the subjacent – already solidified – material. The irradiated regions here correspond to the volume areas of the CAD model. The SLM process includes various exposure strategies which have strong impact on the evolution of the material condition (i.e. residual stresses and porosity), Kruth et al. (2012) and Matsumoto et al. (2002).
- LOWERING: This step characterizes the lowering process of the building platform and thus of the entire powder bed. The most common lowering value here can be found between 30µm and 100µm. The space resulting by the lowering of the platform and the powder bed may be used in the next step for powder deposition.

The SLM process delivers numerous advantages and unique capabilities. For Long-term success and implementation of this technology knowledge and understanding of the mechanisms and influencing factors on the behavior of SLM parts under loading is required. Thus, there is a real need to examine SLM materials. For that reason crack growth analyses on titanium alloy Ti-6-4 and stainless steel AISI 316L were carried out using CT specimens and will be presented in this work.

2. Effect of building direction, heat treatment and build-up rate on fracture mechanical data of laser melted materials

This chapter includes an overview of various influencing factors and their impact on the fracture mechanical values and fatigue crack growth performance of laser melted components. Based on these insights measures for optimization will be taken to get required outcome.

2.1. Sample manufacturing and heat treatment

The materials processed in the current study were Ti-6-4 titanium alloy and AISI 316L stainless steel. The SLM250^{HL} and the SLM280^{HL} facilities were deployed for sample manufacturing – both developed by SLM-Solutions GmbH. These machines allow layer thicknesses ranged between 30µm and 100µm. Compact Tension (CT) specimens with perpendicular as well as parallel initial crack orientation related to the building direction, Fig. 2a,b, were manufactured in order to make conclusions about material isotropy. Fig. 2c illustrates the laser melted plate with dimensions and the final contour of the sample obtained by machining.

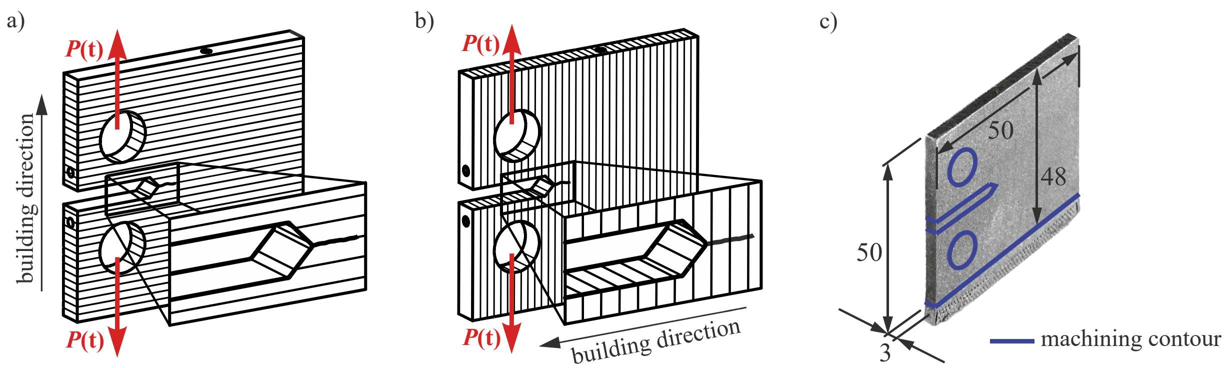

Fig. 2. (a) Building direction normal to crack growth direction, BD⊥CD; (b) Building direction parallel to crack growth direction, BD∥CD; (c) Sample take off by machining from a laser melted plate.

Table 1 contains data of heat treatments that were used in order to modify the As-built material state of CT specimens. These treatments came out of foregoing quasi-static tests (i.e. tensile strength, yield strength and elongation at break) where a wide range of treatments were taken into account, Thöne et al. (2012).

The treatment at 800°C keeps the temperature slightly below the so-called β-transus temperature which means that no change in microstructure occurs. 1050°C treatment is characterized by the exceeding of β-transus temperature and the associated formation of β-phase in titanium microstructure. Thus, after treatment at 1050°C the ratio of β-Ti increases. During the Hot Isostatic Pressure (HIP) the samples remain at 920°C in a chamber filled with argon. Additionally, an isostatic pressure of 1000 bar is applied to the specimens and leads to the reduction of porosity. The result of all treatments is the removal of residual stresses which arise in the melting process.

Table 1. Heat treatment data applied to titanium alloy Ti-6-4.

Heat treatment	800°C	1050°C	HIP
Temperature [°C]	800	1050	920 (1000 bar)
Time [h]	2	2	2
Atmosphere	Argon	Vacuum	Argon

2.2. Titanium alloy Ti-6-4 – effect of building direction and heat treatment on crack growth behavior

The laser melted Ti-6-4 in its untreated condition (As-built) delivers low and insufficient crack growth data, Fig. 3. Heat treatment applications of these parts leads to significantly improved fracture mechanical behavior. Fig. 3a shows the Ti-6-4 crack growth data for laser melted as well as reference material. Fig 3b contains threshold values deduced from *da/dN*-Δ*K*-curves in Fig. 3a. These results indicates that heat treatment is absolutely necessary in order to achieve or even to exceed the threshold values found for Ti-6-4 processed on conventional routes. Currently, heat treatment is the only way to obtain that high level of fracture mechanical performance of Ti-6-4. Further detailed information concerning the fatigue crack growth behavior, the static and fatigue data as well as about the influence of Hot Isostatic Pressing (HIP) on porosity and residual stresses can be found by Leuders et al. (2013).

a)

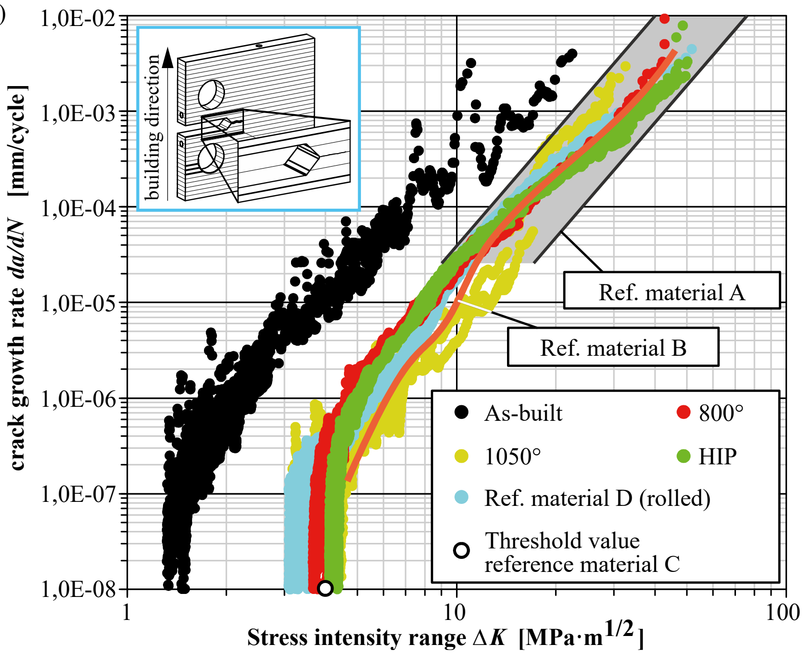

b)

Material condition	Threshold values ΔK_{th} [MPa·m$^{1/2}$]
As-built	1.4
800°C	3.9
1050°C	3.6
HIP	4.2
Ref. material C	4
Ref. material D	3.3

Fig. 3. (a) Fatigue crack growth data for different material conditions (building direction is normal to crack growth direction); (b) Threshold values for the considered material conditions.

Fig. 4 represents a diagram that enables to compare several material conditions under consideration of both static and fatigue crack growth data for two different building directions. The static values are characterized by the yield and tensile strength where the testing direction corresponds to the building direction. The fatigue crack growth values are divided into threshold values (as the limit above that stable crack growth occurs) and into critical stress intensity range (the limit between stable and unstable crack growth). The values presented in Fig. 4 are normalized. For that purpose, each value was related to the maximum value that was found for one of the considered material conditions. Consequently, the values increase from 0 in the middle to the outer line 1 of the plot.

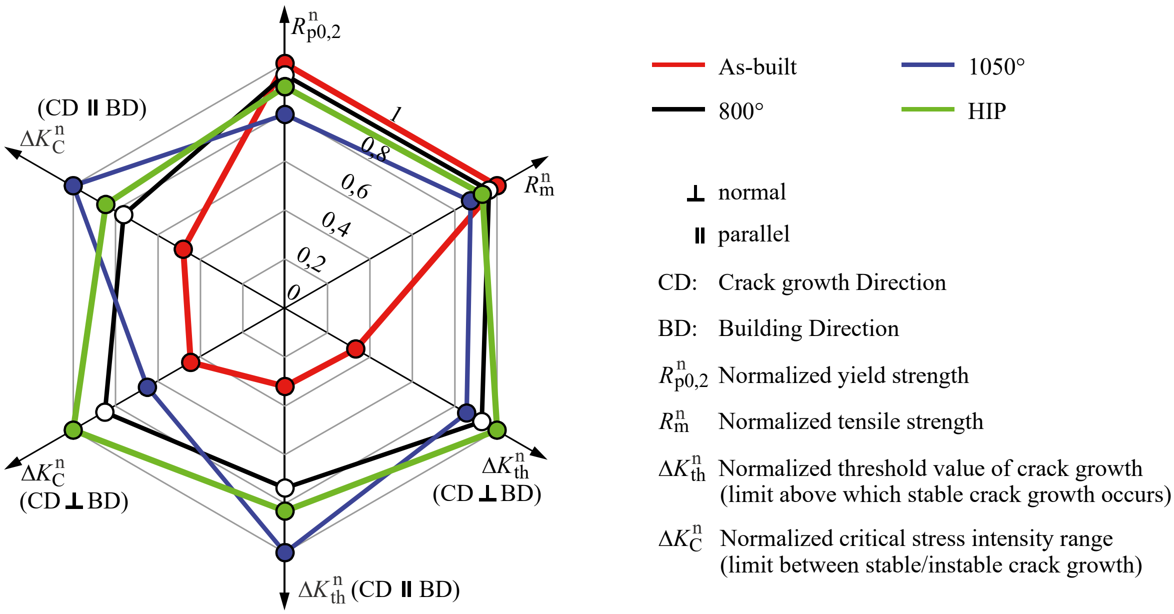

Fig. 4. Comparison of different heat treatments in order to figure out the best suitable post treatment.

The data in Fig. 4 indicates that the heat treatment HIP enables high overall performance in terms of static and fatigue behavior. In conclusion, HIP should be used to obtain the best material performance of laser melted parts consisting of Ti-6-4.

2.3. AISI 316L Stainless steel – effect of build-up rate on crack growth behavior

In this section crack growth data for three different build-up rates will be presented. For this study the laser energy input was varied between 175W and 950W. Depending on the parameter set the theoretical build-up rate could been increased from about 10 cm^3/h to 60 cm^3/h by a factor of six. Fig. 5a contains the *da/dN*-ΔK-curves for the three examined test series. By increasing build-up rate the threshold value decreases here from 3.8 $MPa\cdot m^{1/2}$ for 175 W laser power to 2.4 $MPa\cdot m^{1/2}$ for 950 W laser power. This difference in crack growth data was only established in the lower stress intensity range – near threshold. For PARIS region as well as for the higher stress intensity ranges, approximately identical form and location of *da/dN*-ΔK-curves were obtained for different parameter sets examined in this study, see also Riemer (2015).
Fig. 5b shows the graph where the build-up rate $\dot{V}$, the threshold value ΔK_{th}, the critical stress intensity range ΔK_C, the tensile strength R_m, the yield strength $R_{p0,2}$ and the elongation at break A are plotted as normalized values for the three parameter sets. The increase in the build-up rate leads to a strong decrease in threshold values as well as in elongation at break and a slight decrease in the tensile strength. That means that for higher process productivity the weak material values has to be taken into account. Parts for high performance applications that require high resistance against crack growth have to be processed employing low build-up rates which ensure high-grade properties.

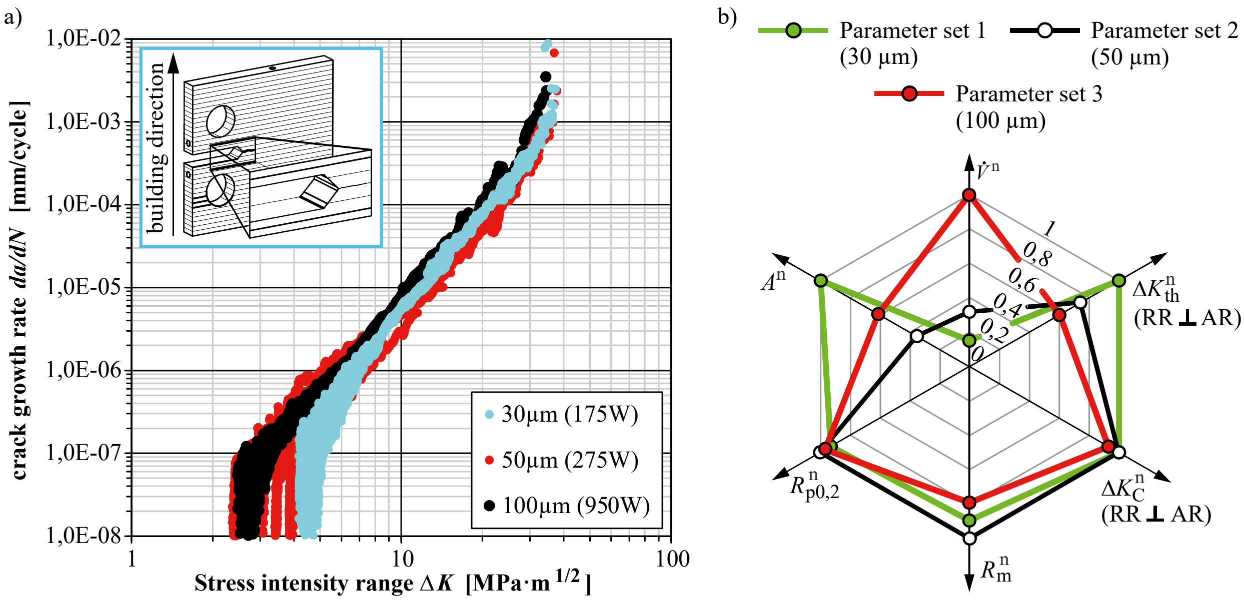

Fig. 5. (a) Fatigue crack growth data depending on the laser power input (build-up rate); (b) Overall material performance depending on the parameter set (build-up rate).

3. Fatigue crack growth in laser melted implants

In this study, the effect of treatment (and consequently of the residual stresses) on the component's lifetime was analyzed. For that reason titanium alloy Ti-6-4 in the conditions As-built and 800° were taken into account. The required fatigue crack growth data, Fig. 6a, was characterized by the FORMAN/METTU-equation as follows:

$$\frac{da}{dN} = C_{\mathrm{FM}} \cdot \left[\left(\frac{1-\gamma}{1-R} \right) \cdot \Delta K_{\mathrm{I}} \right]^{\mathrm{n}} \cdot \frac{\left(1 - \frac{\Delta K_{\mathrm{th}}}{\Delta K_{\mathrm{I}}} \right)^{\mathrm{p}}}{\left(1 - \frac{K_{\mathrm{max}}}{K_{\mathrm{C}}} \right)^{\mathrm{q}}} \quad (1).$$

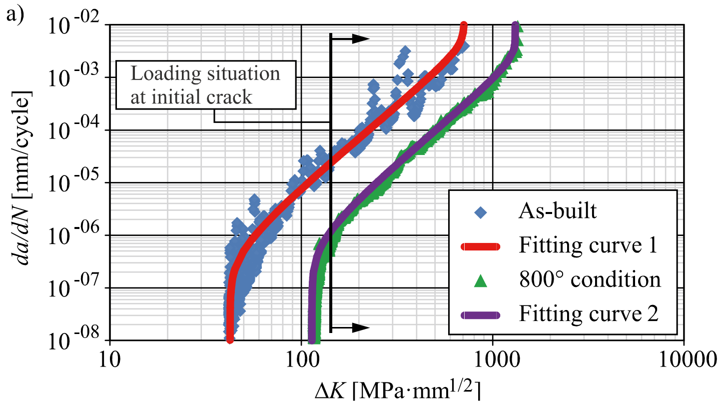

b)

FORMAN/METTU parameter

Parameter	As-built	800°C
C_{FM}	5.00E-11	4.20E-12
γ	0,354647973	0,354647973
R	0.1	0.1
n	2.92	2.92
p	0.5	0.5
q	0.2	0.2
ΔK_{th}	37.2	113.6
K_{C}	660	1460

ΔK_{th} and K_{C} in MPa·mm$^{1/2}$

Fig. 6. (a) FORMAN/METTU-equation fitted to the data for As-built and 800°C conditions; (b) Fitting parameter sets for the FORMAN/METTU-equation.

Fig. 6b contains the parameter sets used to fit the equation (1) to the data for the As-built and 800°C conditions where on the *x*-axis is the crack growth rate in [mm/cycle] and on the *y*-axis is the stress intensity range in [MPa·mm$^{1/2}$]. For detailed information about that equation see also Richard and Sander (2012). In the next step, both mathematical descriptions were implemented into numerical crack growth simulation program ADAPCRACK3D, Schöllmann et al. (2003).

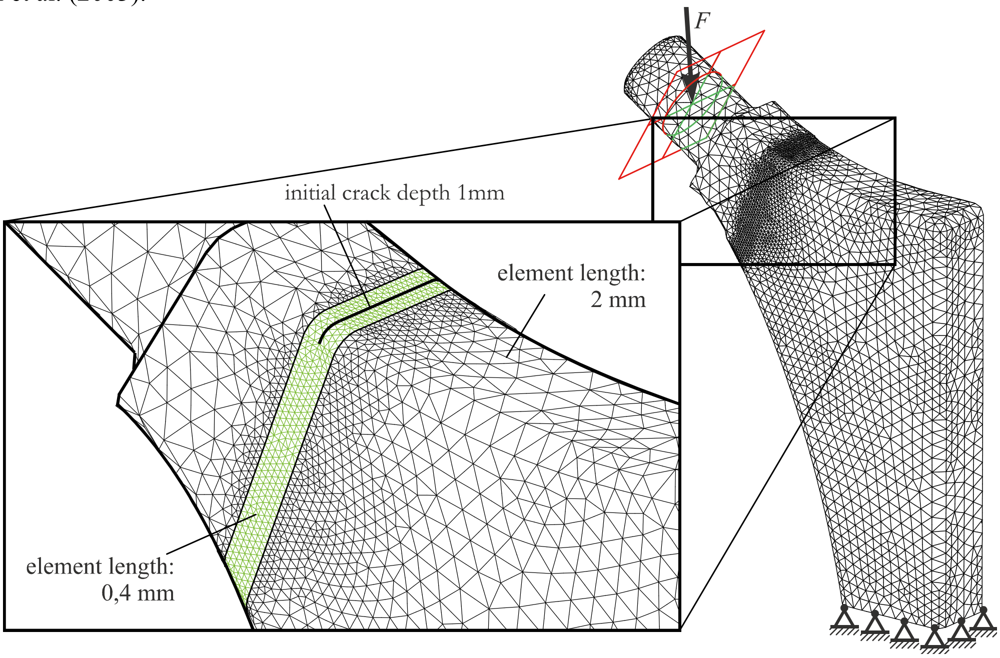

Fig. 7. Boundary conditions and mesh parameters used in numerical simulations for crack growth in the implant.

The object for the lifetime study is the hip joint implant. This part needs to be personalized and consequently well suitable for the production employing the SLM process. The boundary conditions used for the crack growth simulation are presented in Fig. 7 schematically.

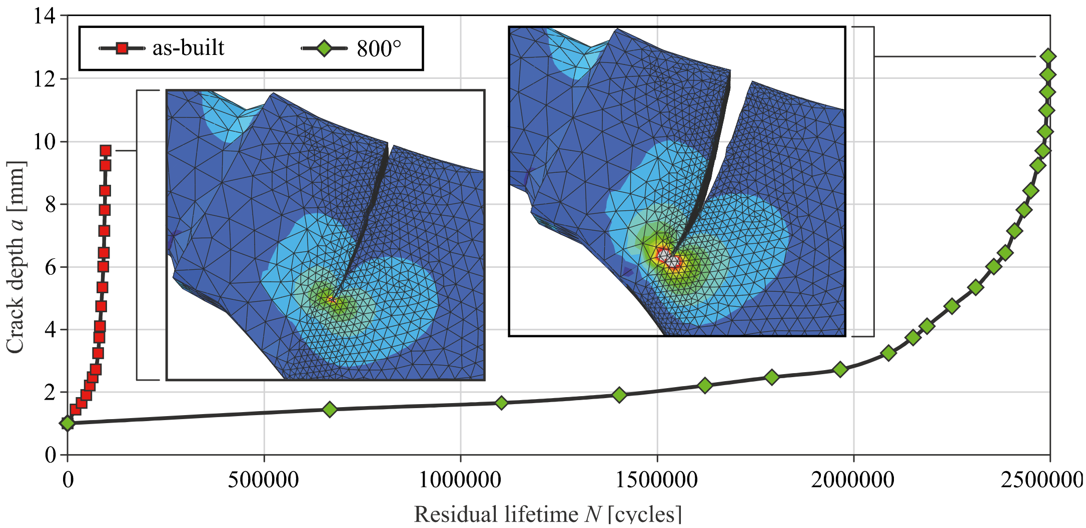

Fig. 8. Numerical simulation of the residual lifetime depending on the material condition.

The boundary conditions used in this study corresponds to the load case "Normal Walking" and are in accordance with the mechanical models developed by Pauwels (1980). The location of the initial crack with a depth of 1 mm was assumed in the region where the highest principal stresses occur, Fig. 7. The *R*-ratio was defined to be 0.1. The simulation was performed based on the body weight of 80 kg. For more details concerning the mesh see also Fig. 7.

Fig. 8 depicts the crack path, the stress distribution and the crack length in the last simulation step before the instable crack growth begins. The results of crack growth simulation show significant differences in the remaining lifetime, c.f. Fig. 8. In the As-built condition the fracture occurs at 100000 cycles. Following the heat treatment at 800°C the instable crack growth begins at 2.5 millions of cycles. Consequently, the treatment at 800°C leads to an huge increase in lifetime. Here, the lifetime extension was found by a factor of about 25. In conclusion, technical parts consisting of Ti-6-4 have to be applied to heat treatment in order to reduce residual stress and to extend the component's lifetime.

References

Gausemeier, J., Echterhoff, N., Kokoschka, M., Wall, M., 2011. Thinking ahead the Future of Additive Manufacturing – Analysis of Promising Industries, Study for the Direct Manufacturing Research Center, Paderborn.

Kruth, J.-P., Leu, M.C., Nakagawa, T., 1998. Progress in Additive Manufacturing and Rapid Prototyping. CIRP Annals - Manufacturing Technology 47, 525–540.

Kruth, J.-P., Deckers, J., Yasa, E., Wauthlé, R., 2012. Assessing and comparing influencing factors of residual stresses in selective laser melting using a novel analysis method. Journal of Engineering Manufacture 226, 980-991.

Leuders, S., Thöne, M., Riemer, A., Niendorf, T., Tröster, T., Richard, H.A., Maier, H.J., 2013. On the mechanical behaviour of titanium alloy TiAl6V4 manufactured by selective laser melting: Fatigue resistance and crack growth performance. International Journal of Fatigue 48, 300-307.

Levy, G.N., Schindel, R., Kruth, J.P., 2003. Rapid manufacturing and rapid tooling with layer manufacturing (LM) technologies, state of the art and future perspectives. CIRP Annals - Manufacturing Technology 52, 589–609.

Matsumoto, M., Shiomi, M., Osakada, K., Abe, F., 2002. Finite element analysis of single layer forming on metallic powder bed in rapid prototyping by selective laser processing. International Journal of Machine & Manufacture 42, 61-67.

Richard, H.A.; Sander, M., 2012. Ermüdungsrisse. Erkennen · Sicher beurteilen · Vermeiden. Springer Vieweg, Wiesbaden.

Riemer, A., 2015. Einfluss von Werkstoff, Prozessführung und Wärmebehandlung auf das bruchmechanische Verhalten von Laserstrahlschmelzbauteilen [Dissertation]. Forschungsberichte des Direct Manufacturing Research Centers, Shaker Verlag, Aachen.

Pauwels, F., 1980. Biomechanics of the Locomotor Apparatus. Contributions on the Functional Anatomy of the Locomotor Apparatus. Springer-Verlag, Berlin Heidelberg New York.

Schöllmann, M., Fulland, M., Richard, H.A., 2003. Development of a new software for adaptive crack growth simulations in 3D structures. Engineering Fracture Mechanics 70, 221-230.

Thöne, M., Leuders, S., Riemer, A., Tröster, T., Richard, H.A., 2012. Influence of heat-treatment on Selective Laser Melting products – e.g. Ti6Al4V. Solid Freeform Fabrication Proceedings, 492-498, Austin.